

Metal Complexes of Cinchonine as Chiral Building Blocks: A Strategy for the Construction of Nanotubular Architectures and Helical Coordination Polymers

Tomasz Kaczorowski,[†] Iwona Justyniak,^{*,‡} Teodozja Lipińska,[§] Janusz Lipkowski,[‡] and Janusz Lewiński^{*,†,‡}

Department of Chemistry, Warsaw University of Technology, Noakowskiego 3, 00-664 Warsaw, Poland, Institute of Physical Chemistry, Polish Academy of Sciences, Kasprzaka 44/52, 01-224 Warsaw, Poland, and Institute of Chemistry, University of Podlasie, 3 Maja 54, 08-110 Siedlce, Poland

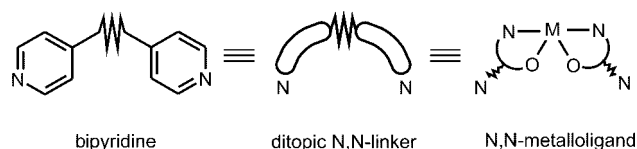
Received December 18, 2008; E-mail: iwona.j@ichf.edu.pl; lewin@ch.pw.edu.pl

During the past two decades, the controlled self-assembly of metal complexes has attracted a great deal of attention because of the potentially wide applications of the resulting supramolecular entities as functional materials.¹ Homochiral porous coordination polymers with nanometer-sized cavities or channels are an important emerging subclass of such materials that are potentially suited for asymmetric catalysis and enantioselective processes.^{1–3} The most common approach for building homochiral supramolecular architectures is the rational combination of chiral multifunctional ligands as linkers and metal ion nodes bearing a specific coordination geometry.¹ This approach, utilizing precoded rigid subunits with the proper bonding and angular information, leads to highly predictable products. However, the engineering of the ligand's features, such as size, flexibility, and directionality of binding centers, is limited by the difficulty of its synthesis. Another level of tailorability in the design of chiral networks can be achieved by implementation of chiral metal–organic complexes as bridging ligands (the so-called metalloligands).^{1c} The general simplicity of preparing new multifunctional building blocks and the capability of generating interesting homo- or heteromultimetallic frameworks are some of the advantages of incorporating metalloligands in the design of functional materials.

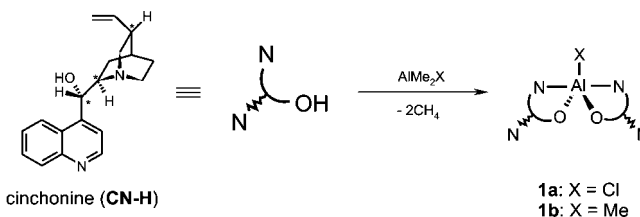
We turned our attention to the surprisingly rarely examined cinchona alkaloid metal complexes,⁴ exploring their utility as chiral building blocks for the construction of homochiral networks; the first robust chiral hybrid organic–inorganic zeolite analogue based on the carboxylic derivative of quinine and its application for enantioseparation of small molecules was reported recently.^{3b,5} Commercially available cinchona alkaloids are widely used in organocatalysis⁶ and occasionally in metal-mediated catalytic processes. For instance, cinchona alkaloids were examined for alkynylzinc asymmetric addition to carbonyl compounds in the presence of $\text{Ti}(\text{O}^i\text{Pr})_4$ ^{7a} or Et_3Al ,^{7b} and a new type of bifunctional catalyst generated from the metal–organic self-assembly of substituted binols and cinchona alkaloids in combination with $\text{Ti}(\text{O}^i\text{Pr})_4$ was developed for the efficient asymmetric hydrophosphonylation of aldehydes.⁸

Following our recent report on a simple combination of R_2Zn compounds and bipyridines leading to a novel class of organometallic coordination polymers of unique topology,⁹ we became highly encouraged to replace common bipyridines as N-ditopic organic linkers¹⁰ by metal complexes with pyridyl units (Scheme 1). We describe here our initial results on the synthesis and characterization of the first cinchonine-based metalloligands and demonstrate their excellent capability for noncovalent-interaction-driven self-assembly

Scheme 1. Strategy for Developing Novel N-Ditopic Linkers



Scheme 2



into novel helical nanotubular architectures as well as the utility of their coordination-driven self-organization for constructing chiral coordination polymers.

Our primary attempts to isolate titanium derivatives of cinchonine (CN-H) failed,¹¹ so as a next step we turned our attention to the corresponding aluminum complexes. The reaction of AlMe_2Cl or AlMe_3 with 2 equiv of CN-H afforded the bischelat complexes $(\text{CN})_2\text{AlX}$ [X = Cl (**1a**), Me (**1b**)] in essentially quantitative yield (Scheme 2). The two complexes were isolated by crystallization from toluene (**1a**) or THF (**1b**) solution as colorless needlelike crystals suitable for X-ray analysis; they crystallized in the chiral trigonal space group $P3_112$ with Flack parameters close to zero [see the Supporting Information (SI)]. **1a** and **1b** are isostructural monomeric five-coordinate aluminum complexes sustained by one X group and two chelating cinchonine ligands (Figure 1a and Figures 1S and 2S in the SI).¹² The aluminum centers adopt distorted trigonal bipyramidal geometries with O and X at the equatorial positions and quinuclidine N atoms at the axial positions (the corresponding geometric parameters of **1a** and **1b** are essentially similar). A more detailed analysis of the supramolecular structures of **1a** and **1b** shows a richness of inspiring unique features. In both compounds, $(\text{CN})_2\text{AlX}$ molecules are organized through noncovalent interactions into extended quasi-honeycomb networks with homochiral one-dimensional (1D) tubular channels (Figure 1c). The average inner diameter of the channels is ~ 8 Å, and the free space is filled by the solvent molecules (Figure 2). On the basis of PLATON calculations,¹³ the open channels constitute about 36.0% (2513.4 of 6980.4 Å³) and 37.5% (2678.4 of 7147.8 Å³) of the crystal volumes of **1a** and **1b**, respectively.¹⁴ Particularly fascinating is the pattern in which the tubular architecture is organized. The $(\text{CN})_2\text{AlX}$ molecules are arranged in a right-handed

[†] Warsaw University of Technology.

[‡] Polish Academy of Sciences.

[§] University of Podlasie.

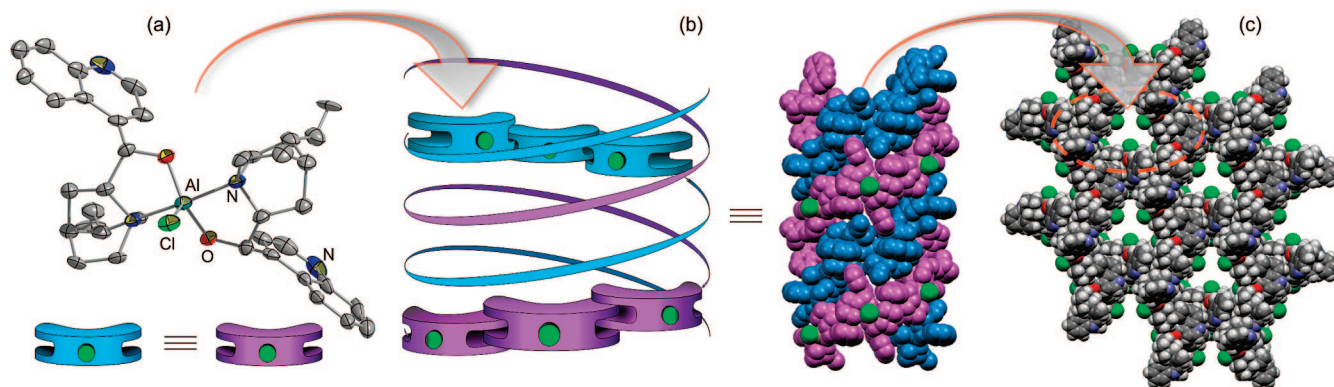


Figure 1. Graphical representation of the self-organization process of the metalloligand **1a** into the honeycomb network with homochiral 1D tubular channels.

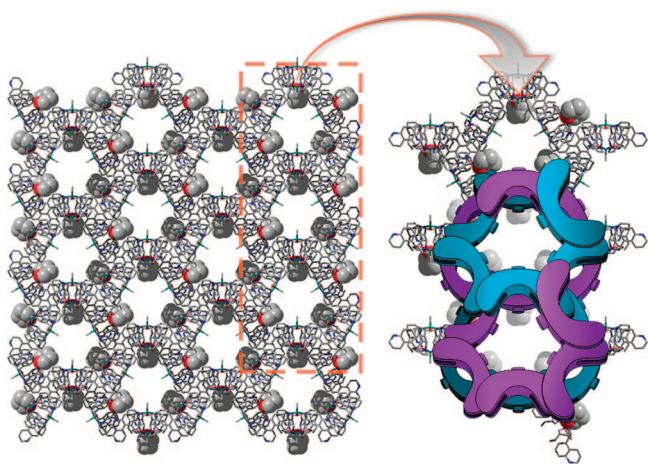


Figure 2. 1D nanotubes of **1b** along the *c* axis with entrapped THF molecules.

double-helical motif in which each strand is generated by C–H⋯ π -bonded monomeric moieties connected to adjacent strand by the same class of interactions. The complete cycle in each strand contains six (CN)₂AlX units with a pitch of 22.35 Å. Moreover, the (CN)₂AlX complexes utilize their unique shape to form helical chains in two different modes. In the two cases, the pattern is analogous: the cavity between the quinuclidine and quinoline moieties of the cinchonine ligand is partially filled by a quinuclidine or quinoline residue from the neighboring (CN)₂AlX unit. However, one arrangement mode (the “in” mode) leads to a chain with the Al–X bonds facing toward the inside of the channel, while in the second mode (the “out” mode), the same type of bonds are oriented outward (Figure 1b). Thus, the shape of (CN)₂AlX molecules drives their unique self-organization pattern, which resembles a hingelike mechanism that operates by switching between the “in” and “out” modes. Another interesting feature is that each (CN)₂AlX unit is shared between two neighboring helices, giving rise to the extended 3D network. The channels’ inner diameter varies in the range ~7–9 Å in response to the helical arrangement of the X substituents inside the channels. We note that crystallization of **1b** from (±)-2-methyltetrahydrofuran (Me-THF) did not affect the structure of the resulting framework (see below). The above results demonstrate the inherent propensity of (CN)₂AlX to utilize its molecular shape in noncovalent-interaction-driven self-assembly into chiral tubular architectures regardless of both the X substituent at Al center and the employed solvent. This observation is striking, as only a few examples of chiral nanotubular assemblies involving metal complexes have been reported to date.^{3f,15}

Thermogravimetric analysis (TGA) showed that the release of toluene molecules from polycrystalline **1a** was completed by 140 °C. Moreover, the experimental powder X-ray diffraction patterns obtained from the resulting microcrystalline samples of **1a** (Figure 3S in the SI) show that the release of toluene molecules is accompanied by a transition to a new crystalline phase having an as yet unidentified structure, and this new framework is maintained until 220 °C. The resulting solid product **1a'** is essentially nonporous to nitrogen and has a very low BET surface area (1.74 m² g^{−1}; see Figure 4S in the SI). Surprisingly, THF gradually leaves the porous network of **1b** up to ~220 °C (for the TGA profile, see Figure 5S in the SI) with the loss of crystallinity, and the resulting amorphous material is nonporous, as indicated by the N₂ sorption experiment. The numbers of encapsulated solvent molecules per (CN)₂AlX molecule (estimated from TGA and ¹H NMR data) are 2 and 1 for **1a** and **1b**, respectively.

Resolution of enantiomers through selective crystallization of diastereomeric inclusion compounds mediated by porous coordination polymers remains a challenging task.³ One can envisage that the observed high propensity of (CN)₂AlX complexes to form chiral cavities by interdigitated gear faces, along with the helical arrangement of exposed electronegative atoms inside the channels (such as Cl atoms in **1a**), has potential value for the formation of inclusion compounds that discriminate between chiral guests. An additional advantage would be that products could be extracted by facile disassembly followed by host regeneration. Thus, we arranged an experiment to test whether a (CN)₂AlX system is capable of resolving an organic racemate by a two-step process involving inclusion crystallization of an (CN)₂AlX host in a mixture of the racemic guest followed by removal of the guest under reduced pressure. Complex **1b** was dissolved in Me-THF and then crystallized from this solvent, and single crystals were collected for X-ray analysis. The crystal structure analysis revealed that the replacement of the THF solvent by Me-THF did not affect the supramolecular architecture of the resulting framework. The only difference was that the channels were filled by Me-THF molecules in disorder (see Figure 2S in the SI). Optical rotatory power measurements on the recovered Me-THF showed a small enantiomeric enrichment of ~7% ee. As anticipated, after removal of the guest, crystals of **1b** could be recycled and again utilized for the enrichment of another batch of Me-THF.

Complexes **1a** and **1b** contain two quinoline N centers capable of further coordination to metal centers; the quinoline rings are oriented in nearly parallel fashion with the N atoms ~10.2 Å away from each other, and the links form an angle of ~69°. These features, together with the bulkiness and relative rigidity of the carbon backbones, make this type of complex a potential N,N-

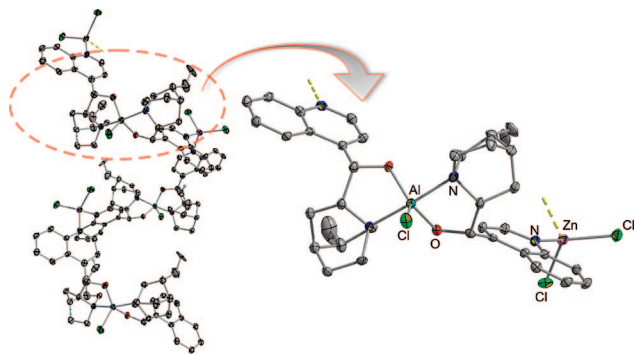


Figure 3. Helical 1D coordination polymer formed by **1a** and ZnCl_2 .

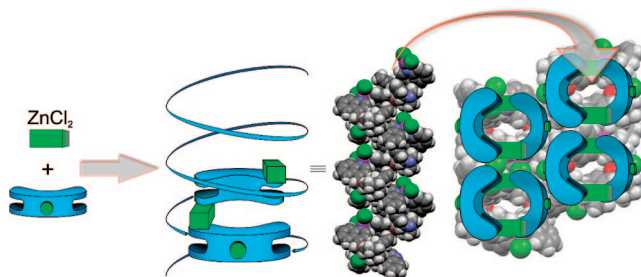


Figure 4. Graphical representation of helical architectures based on the metalloligand **1a** and ZnCl_2 .

ditopic metalloligand for the construction of chiral homo- or heterometallic coordination polymers, as confirmed by a further control experiment. Upon very slow addition of ZnCl_2 in THF to a solution of **1a** in THF, a white precipitate of **2** was deposited, from which single crystals were collected for X-ray analysis. The molecular structure of **2** consists of $(\text{CN})_2\text{AlCl}$ units with ZnCl_2 moieties coordinated to the quinoline N centers (Figure 3).

From the analysis of bond distances and angles, one can conclude that the reaction did not lead to significant changes in the geometrical parameters of **1a**. The tetrahedral coordination of each Zn center is completed by another quinoline N atom from a neighboring **1a** molecule. Thus, the reaction virtually led from unzipping of the $\text{C}-\text{H}\cdots\pi$ -bonded double-helical structure of **1a** to a 1D bimetallic coordination polymer of helical topology (Figure 4). The helical pitch is 13.86 Å, with two **1a**– ZnCl_2 units per cycle. The helices are close-packed, generating a network of 1D channels filled by THF molecules. Each channel (with an average inner diameter of ~ 5 Å and a void volume of 24.2%, as calculated by PLATON) runs helically, interweaving with metal–organic chains as a complementary second helical strand. A more thorough analysis of the helical structure of **2** led to the striking conclusion that employing ZnCl_2 as a connector allowed for the inversion of the helix handedness, which passed from right-handed helix in **1a** to left-handed in **2**. Therefore, the handedness of **1a**-derived helices is not an intrinsic property of chiral **1a** or the cinchonine precursor, as we have demonstrated that control over the handedness can be achieved by changing the mode in which **1a** units are connected.

In conclusion, the results demonstrate a viable means of constructing novel chiral N-ditopic metalloligands, from which new chiral nanotubular architectures through noncovalent-interaction-driven self-assembly as well as new 1D bimetallic coordination polymers of helical topology can be formed. The disclosed high propensity of bischelate metal complexes derived from easily accessible cinchona alkaloids to form chiral cavities in interdigitated gear faces provides new opportunities for designing enantioselective

processes that would occur in crystalline solids. Efforts to extend this strategy to other cinchona alkaloid ligands and metal centers to produce novel, controllable chiral supramolecular architectures with tailor-made properties, including enantioselective recognition and separation, are underway.

Acknowledgment. This work was supported by the State Committee for Scientific Research (Grants 3 T09B 037 28, PBZ-KBN-117/T08/06, and PBZ-KBN-118/T09/04).

Supporting Information Available: Additional experimental, spectroscopic, TGA, and N_2 sorption data and crystallographic data in CIF format. This material is available free of charge via the Internet at <http://pubs.acs.org>.

References

- (1) For selected reviews, see: (a) Leininger, S.; Olenyuk, B.; Stang, P. J. *Chem. Rev.* **2000**, *100*, 853. (b) Holliday, B. J.; Mirkin, C. A. *Angew. Chem., Int. Ed.* **2001**, *40*, 2022. (c) Kesanli, B.; Lin, W. *Coord. Chem. Rev.* **2003**, *246*, 305. (d) Janiak, C. *Dalton Trans.* **2003**, 2781. (e) Kitagawa, S.; Kitaura, R.; Noro, S. *Angew. Chem., Int. Ed.* **2004**, *43*, 2334. (f) Dai, L. X. *Angew. Chem., Int. Ed.* **2004**, *43*, 5726. (g) Ockwig, N. W.; Delgado-Friedrichs, O.; O'Keefe, M.; Yaghi, O. M. *Acc. Chem. Res.* **2005**, *38*, 176. (h) Bradshaw, D.; Claridge, J. B.; Cussen, E. J.; Prior, T. J.; Rosseinsky, M. J. *Acc. Chem. Res.* **2005**, *38*, 273. (i) Férey, G. *Chem. Soc. Rev.* **2008**, *37*, 191. (j) Suh, M. P.; Cheon, Y. E.; Lee, E. Y. *Coord. Chem. Rev.* **2008**, *252*, 1007.
- (2) Selected examples: (a) Seo, J. S.; Whang, D.; Lee, H.; Jun, S. I.; Oh, J.; Jeon, Y. J.; Kim, K. *Nature* **2000**, *404*, 982. (b) Wu, C. D.; Hu, A.; Zhang, L.; Lin, W. *J. Am. Chem. Soc.* **2005**, *127*, 8940. (c) Dybtsev, D. N.; Nuzhdin, A. L.; Chun, H.; Bryliakov, K. P.; Talsi, E. P.; Fedin, V. P.; Kim, K. *Angew. Chem., Int. Ed.* **2006**, *45*, 916. (d) Cho, S.-H.; Ma, B.; Nguyen, S. T.; Hupp, J. T.; Albrecht-Schmitt, T. E. *Chem. Commun.* **2006**, 2563. (e) Wu, C. D.; Lin, W. *Angew. Chem., Int. Ed.* **2007**, *46*, 1075.
- (3) (a) Kepert, C. J.; Prior, T. J.; Rosseinsky, M. J. *J. Am. Chem. Soc.* **2000**, *122*, 5158. (b) Xiong, R. G.; You, X. Z.; Abrahams, B. F.; Xue, Z.; Che, C. M. *Angew. Chem., Int. Ed.* **2001**, *40*, 4422. (c) Bradshaw, D.; Prior, T. J.; Cussen, E. J.; Claridge, J. B.; Rosseinsky, M. J. *J. Am. Chem. Soc.* **2004**, *126*, 6106. (d) Song, Y. M.; Zhou, T.; Wang, X. S.; Li, X. N.; Xiong, R. G. *Cryst. Growth Des.* **2006**, *6*, 14. (e) Vaidhyanathan, R.; Bradshaw, D.; Rebilly, J. N.; Barrio, J. P.; Gould, J. A.; Berry, N. G.; Rosseinsky, M. J. *Angew. Chem., Int. Ed.* **2006**, *45*, 6495. (f) Li, G.; Yu, W.; Cui, Y. *J. Am. Chem. Soc.* **2008**, *130*, 4582. (g) Li, G.; Yu, W.; Ni, J.; Liu, T.; Liu, Y.; Sheng, E.; Cui, Y. *Angew. Chem., Int. Ed.* **2008**, *47*, 1245.
- (4) (a) Tesarowicz, I.; Oleksyn, B. J.; Nitek, W. *Chirality* **2007**, *19*, 152. (b) Qu, Z. R.; Chen, Z. F.; Zhang, J.; Xiong, R. G.; Abrahams, B. F.; Xue, Z. L. *Organometallics* **2003**, *22*, 2814. (c) Wang, G. X.; Xiong, R. G. *Chin. J. Chem.* **2007**, *25*, 1405. (d) Hubel, R.; Polborn, K.; Beck, W. *Eur. J. Inorg. Chem.* **1999**, 471.
- (5) For the chirality induction effect of cinchona alkaloids on homochiral crystallization of metal–organic frameworks from achiral precursors, see: Zhang, J.; Chen, S.; Wu, T.; Feng, P.; Bu, X. *J. Am. Chem. Soc.* **2008**, *130*, 12882.
- (6) Kacprzak, K.; Gawroński, J. *Synthesis* **2001**, 961.
- (7) (a) Kamble, R. M.; Singh, V. K. *Tetrahedron Lett.* **2003**, *44*, 5347. (b) Liu, L.; Wang, R.; Kang, Y. F.; Chen, C.; Xu, Z. Q.; Zhou, Y. F.; Ni, M.; Cai, H. Q.; Gong, M. Z. *J. Org. Chem.* **2005**, *70*, 1084.
- (8) Yang, F.; Zhao, D.; Lan, J.; Xi, P.; Yang, L.; Xiang, S.; You, J. *Angew. Chem., Int. Ed.* **2008**, *47*, 5646.
- (9) Lewiński, J.; Dranka, M.; Bury, W.; Śliwiński, W.; Justyniak, I.; Lipkowski, J. *J. Am. Chem. Soc.* **2007**, *129*, 3096.
- (10) For reviews, see: (a) Kaes, C.; Katz, A.; Hosseini, M. W. *Chem. Rev.* **2000**, *100*, 3553. (b) Biradha, K.; Sarkar, M.; Rajput, L. *Chem. Commun.* **2006**, 4169. (c) Barnett, S. A.; Champness, N. R. *Coord. Chem. Rev.* **2003**, *246*, 145.
- (11) The reaction of $\text{Ti}(\text{O}^i\text{Pr})_4$ with 2 equiv of cinchonine in toluene solution was carried out and afforded a complex mixture that was difficult to separate and characterize.
- (12) For the first structurally authenticated bischelate alkylaluminum derivative of an aminoalcohol, see: Gelbrich, T.; Hecht, E.; Thiele, K. H.; Sieler, J. *J. Organomet. Chem.* **2000**, *595*, 21. For a bischelate chloroaluminum derivative of a chiral aminophenol, which was applied in an asymmetric Mukaiyama–Michael reaction, see: Takenaka, N.; Abell, J. P.; Yamamoto, H. *J. Am. Chem. Soc.* **2007**, *129*, 742.
- (13) Spek, A. L. *J. Appl. Crystallogr.* **2003**, *36*, 7.
- (14) For the seminal paper concerning realistic values of porosity in microporous materials, see: Soldatov, D. V.; Moudrakovskii, I. L.; Grachev, E. V.; Ripmeester, J. A. *J. Am. Chem. Soc.* **2006**, *128*, 6737.
- (15) (a) Orr, G. W.; Barbour, L. J.; Atwood, J. L. *Science* **1999**, *285*, 1049. (b) Cui, Y.; Lee, S. J.; Lin, W. *J. Am. Chem. Soc.* **2003**, *125*, 6014. (c) Hao, X. R.; Wang, X. L.; Qin, C.; Su, Z. M.; Wang, E. B.; Lan, Y. Q.; Shao, K. Z. *Chem. Commun.* **2007**, 4620. (d) Heo, J.; Jeon, Y. M.; Mirkin, C. A. *J. Am. Chem. Soc.* **2007**, *129*, 7712.

JA8098867